PROCEEDINGS OF SPIE

SPIEDigitalLibrary.org/conference-proceedings-of-spie

Giant second-harmonic generation in photonic crystal slabs possessing double-resonance bound states in the continuum

Ji Tong Wang, Fengxia Li, Nicolae Panoiu

Ji Tong Wang, Fengxia Li, Nicolae C. Panoiu, "Giant second-harmonic generation in photonic crystal slabs possessing double-resonance bound states in the continuum," Proc. SPIE 12405, Nonlinear Frequency Generation and Conversion: Materials and Devices XXII, 124050K (14 March 2023); doi: 10.1117/12.2653320

SPIE.

Event: SPIE LASE, 2023, San Francisco, California, United States

Giant second-harmonic generation in photonic crystal slabs possessing double-resonance bound states in the continuum

Ji Tong Wang[a], Fengxia Li[b], and Nicolae C. Panoiu[a]

[a]Department of Electronic and Electrical Engineering, University College London, Torrington Place, London, United Kingdom
[b]School of Physics and Optoelectronic Engineering, Xidian University, No. 2 South Taibai Road, Xian, China

ABSTRACT

The ability to confine and guide light makes photonic crystals (PhCs) a promising platform for large local field enhancement, which enables efficient nonlinear processes at the nanoscale. Here, we utilize optical bound states in the continuum (BICs) to engineer sharp resonances with high quality factors. By investigating the angle-resolved reflection spectra, we demonstrate that two PhC slabs with different configuration but the same lattice constant support a pair of at-Γ and a pair of off-Γ resonances, respectively. In both cases, BIC-type resonances are observed at the fundamental frequency while BIC-like resonances are found at the second harmonic. This double-resonance phenomenon is subsequently used to significantly enhance the second-harmonic generation from PhC slabs. The maximum values of the SHG are several orders of magnitude larger than those corresponding to the reference slabs. We consider that our approach based on double-resonance BICs provides a novel way to realize enhanced harmonic generation in photonic nanodevices.

Keywords: Bound states in the continuum, second-harmonic generation, nanophotonics, photonic crystal slabs

1. INTRODUCTION

Optical bound states in the continuum (BICs) are localized optical modes situated inside of the continuum spectrum of a photonic structure, and which do not radiate into the far field.[1–3] As a consequence of these properties, they manifest themselves as resonances with infinite quality factor (Q-factor). In general, an open periodic optical system can support two types of BICs: symmetry-protected BICs arising from symmetry mismatch between the eigenmodes of the optical system and radiative channels, and accidental BICs, which are achieved through structural parameter tuning. Thanks to the ability to manipulate the optical field, a plethora of practical applications have been explored in nanophotonics within the past decade, ranging from sensing[4,5] and lasing[6,7] to nonlinear optics.[8,9] Based on the radiation-free property of BICs, they provide promising routes to achieve enhanced light-matter interaction in optical nanostructures, such as photonic crystal (PhC) slabs.

In this work, we report that, by utilizing symmetry mismatch and parameter tuning, BICs can be realized at the fundamental frequency (FF) while BIC-like resonances with high Q-factors can be achieved at the second-harmonic (SH), that is above the diffraction limit of periodic PhC slabs. The BIC-like resonances are coupled with BICs through the second-order optical nonlinearity of the PhC slab,[10–12] assumed to be made of silicon nitride (SiN), thus producing a strong enhancement of the SHG. Taking advantage of this mechanism, SHG is increased by several orders of magnitude as compared to that radiated by the reference PhC slabs.

Further author information: (Send correspondence to Nicolae C. Panoiu)
Nicolae C. Panoiu: E-mail: n.panoiu@ucl.ac.uk

Nonlinear Frequency Generation and Conversion: Materials and Devices XXII,
edited by Peter G. Schunemann, Proc. of SPIE Vol. 12405, 124050K
 · 0277-786X · doi: 10.1117/12.2653320

2. LINEAR OPTICAL RESPONSE OF THE PHOTONIC CRYSTAL SLABS

We consider two PhC slabs with different configurations but the same lattice constant, $a = 995\,\text{nm}$, the schematics being illustrated in Fig. 1(a). For the sake of specificity, we assume that both PhC slabs are made of SiN with a refractive index of 1.94 at the FF and 1.98 at the SH, as they were experimentally measured.[13] The first design of the PhC slab has hole radius, $r = 236\,\text{nm}$, and slab thickness, $d = 528\,\text{nm}$, and supports a pair of resonances at a high symmetry point (Γ point), while the second PhC slab has $r = 128\,\text{nm}$ and $d = 678\,\text{nm}$ and possesses a pair of resonances at certain points in the reciprocal space.

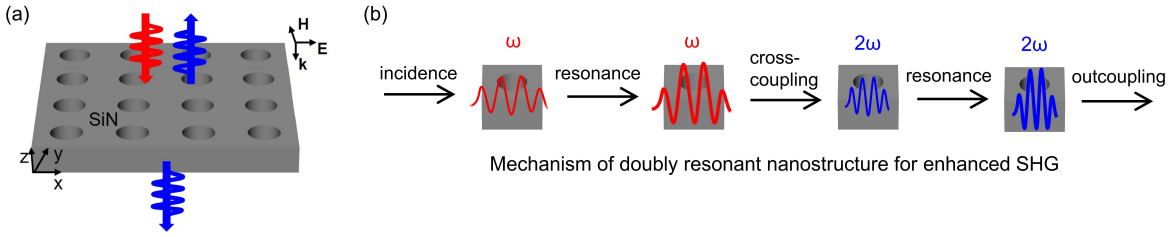

Figure 1. (a) The schematics of the mechanism for second-harmonic generation from a SiN photonic crystal slab consisting of a square array of air holes, under the excitation of plane waves. (b) The step-by-step mechanism of second-harmonic generation enhancement via double-resonance excitation phenomenon in nanostructures, where ω (2ω) denotes the fundamental frequency (second-harmonic).

The physical mechanism of a double-resonance phenomenon in photonic nanostructures for enhanced SHG is illustrated in Fig. 1(b). At the FF, an optical resonance couples to the incoming waves, so as to increase the local linear optical field. Then, the cross-coupling between this optical mode at the FF and the generated field at the SH, mediated by the second-order nonlinear optical susceptibility of the medium, leads to further enhancement of the SHG.

Next, the reflection maps calculated numerically using the rigorous coupled-wave analysis method[14] are shown in Figs. 2(a)-2(d), for both pairs of resonances. Regarding the at-Γ resonance pair [Figs. 2(a) and 2(c)], a symmetry-protected BIC, denoted by BIC 1, is found at 200.5 THz. Its complete decoupling from the radiative continuum gives leads to an infinite Q-factor. To utilize the double-resonance effect, another resonance, denoted by $R3$, with a small line width at the Γ point is observed at 401 THz. Its finite and particularly large Q-factor at the angle of incidence of $\theta = 0$ can be explained by the existence of additional diffraction channels since the frequency of $R3$ is beyond the diffraction limit, $f_0 = c_0/n_{air}a \approx 300\,\text{THz}$, where c_0 is the speed of light in vacuum.

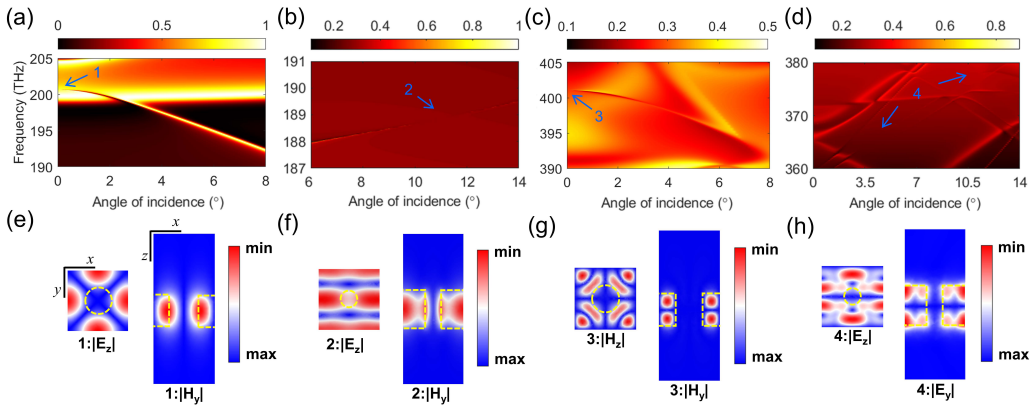

Figure 2. (a)-(d) Reflection maps for BIC 1, BIC 2, BIC-like $R3$, and BIC-like $R4$, respectively. The blue arrows indicate their location in the spectral dispersion maps. (e)-(h) The corresponding field profiles for all four resonances within a unit cell calculated at the marked points. For $R4$, the field at $\theta = 4^\circ$ is shown.

As a result, four first-order diffraction channels open. However, the zeroth diffraction order is still protected by the in-plane inversion symmetry of the PhC slab and the suppression of radiation into this diffraction channel accounts for the high Q-factor of $R3$.

We also studied the optical response of the pair of off-Γ resonances, as per Figs. 2(b) and 1(d). An accidental BIC, denoted by BIC 2, stemming from destructive interference occurs when $\theta = 11.1°$. In the vicinity of the double the frequency of BIC 2, another resonance, called $R4$, whose line width is vanishingly small when the angle of incidence is equal to 4° and 10.5°. The BIC 2 is expected to nonlinearly couple to $R4$ at around $\theta = 11°$ where the phase-matching condition is satisfied. Overall, $R4$ allows for five diffraction channels, and the underlying physics for its high Q factor can be traced to the interference between these different diffraction channels. For BIC 1, BIC 2, and $R3$, transverse-magnetic polarized plane wave is applied as a pump field, whereas transverse-electric polarized plane wave is used to excite $R4$. In order to gain deeper physical insights, the field distributions for all four resonances are shown in Figs. 2(e)-2(h). Clearly, for all four resonances, there can be observed a strong field confinement across the PhC slab (z-axis).

3. ENHANCED SECOND-HARMONIC GENERATION FROM DOUBLE-RESONANCE BICS

In the last part of our study, we used the mechanism of double-resonance BICs to illustrate the giant enhancement of SHG in our PhC slabs. To this end, we consider the second-order nonlinear polarization, which can be expressed as

$$\mathbf{P}^{(2)}(\mathbf{r}, 2\omega) = \epsilon_0 \boldsymbol{\chi}^{(2)}(\mathbf{r}; 2\omega, \omega, \omega) : \mathbf{E}(\mathbf{r}, \omega)\mathbf{E}(\mathbf{r}, \omega), \tag{1}$$

where $\mathbf{P}^{(2)}(\mathbf{r}, 2\omega)$ is the nonlinear polarization at the SH, $\mathbf{E}(\mathbf{r}, \omega)$ is the electric field applied at the FF, and $\boldsymbol{\chi}^{(2)}$ is the second-order susceptibility tensor. For SiN (symmetry group $C_{\infty v}$), the non-vanishing second-order susceptibility tensor components are $\chi_{xxz} = \chi_{xzx} = \chi_{yyz} = \chi_{yzy} = 0.4\,\text{pm/V}$, $\chi_{zxx} = \chi_{zyy} = 0.34\,\text{pm/V}$, and $\chi_{zzz} = 1.1\,\text{pm/V}$, where x- and y-axis are in the plane of the slab and the z-axis is perpendicular onto it.[13]

For the pair of at-Γ resonances (BIC 1 and $R3$), we show in Fig. 3(a) the dispersion map of normalized SHG intensity, whereby the evolution of two peaks marked as white dashed lines can be observed. They correspond to the dependence on the angle of incidence of the resonance frequencies of BIC 1 and $R3$. For the BIC-induced peak, one can understand the origin of the enhanced SHG as the intense light-matter interaction at the FF. For the other peak, the underlying physics can be traced to the resonant effects at the SH. The two peaks coincide when the angle of incidence is equal to 0°, thus the maximum SHG is expected to be emitted near normal incidence. To quantify this enhancement effect, we used the SHG intensity at normal incidence as a reference, and observed that the enhancement ratio η is as large as eight orders of magnitude at 401 THz when $\theta = 0.1°$ – see Fig. 3(c). Furthermore, one can also achieve resonantly increased SHG from the double-resonance BICs,

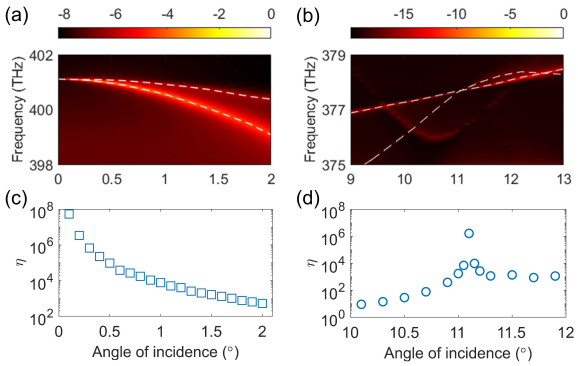

Figure 3. (a),(b) The dispersion maps of normalized SHG intensity for the at-Γ and off-Γ pairs of resonances, respectively, whereby the white dashed lines show the angle-dependent resonance dispersion of SHG. (c),(d) The evolution of enhancement ratio η with respect to the angle of incidence, determined for the two pairs of resonances. See the text for the definition of the reference SHG intensity in the two cases.

BIC 2 and $R4$, at the off-Γ point previously determined. To illustrate this, we plot in Fig. 3(b) the dispersion map of normalized SHG intensity with respect to θ. We stress that the nonlinear polarization generated by BIC 2 can not directly couple to $R4$ as the symmetry properties of the system forbid this nonlinear interaction. To overcome this constraint, we utilize the well-known technique of periodic poling of the nonlinear susceptibility, $\chi^{(2)}$. Then, the largest enhancement of SHG is achieved at the double-resonance cross point, namely at $\theta = 11.1°$. The SHG intensity before nonlinear poling is used as a reference to quantify the enhancement effect, and the largest enhancement ratio η reaches 10^7, as per Fig. 3(d).

4. CONCLUSION

In conclusion, we utilize the physics of BICs, for both symmetry-protected and accidental BICs, to engineer high-Q resonances at both the fundamental frequency and second harmonic. Using this double-resonance phenomenon, second-harmonic generation is enhanced by several orders of magnitude as compared to that obtained in the reference, off resonance, PhC slab. Importantly, the results presented here provide a novel recipe for the realization of harmonic generation and expand the scope of the BIC-based applications in nonlinear wave generation and topological physics.

ACKNOWLEDGMENTS

The authors acknowledge financial support from European Research Council (ERC- 2014-CoG-648328) and China Scholarship Council.

REFERENCES

[1] Marinica, D. C., Borisov, A. G., and Shabanov, S. V., "Bound states in the continuum in photonics," *Phys. Rev. Lett.* **100**, 183902 (2008).

[2] Zhen, B., Hsu, C. W., Lu, L., Stone, A. D., and Soljacic, M., "Topological nature of optical bound states in the continuum," *Phys. Rev. Lett.* **113**, 257401 (2014).

[3] Hsu, C. W., Zhen, B., Stone, A. D., Joannopoulos, J. D., and Soljačić, M., "Bound states in the continuum," *Nat. Rev. Mater.* **1**, 16048 (2016).

[4] Azzam, S. I. and Kildishev, A. V., "Photonic bound states in the continuum: From basics to applications," *Adv. Opt. Mater.* **9**, 2001469 (2020).

[5] Wang, Y., Han, Z., Du, Y., and Qin, J., "Ultrasensitive terahertz sensing with high-Q toroidal dipole resonance governed by bound states in the continuum in all-dielectric metasurface," *Nanophotonics* **10**, 1295–1307 (2021).

[6] Yu, Y., Sakanas, A., Zali, A. R., Semenova, E., Yvind, K., and Mørk, J., "Ultra-coherent fano laser based on a bound state in the continuum," *Nat. Photonics* **15**, 758–764 (2021).

[7] Zhang, X., Liu, Y., Han, J., Kivshar, Y., and Song, Q., "Chiral emission from resonant metasurfaces," *Science* **377**, 1215–1218 (2022).

[8] Koshelev, K., Tang, Y., Li, K., Choi, D.-Y., Li, G., and Kivshar, Y., "Nonlinear metasurfaces governed by bound states in the continuum," *ACS Photonics* **6**, 1639–1644 (2019).

[9] Jin, J., Lu, J., and Zhen, B., "Resonance-forbidden second-harmonic generation in nonlinear photonic crystals," *Nanophotonics* **10**, 4233–4239 (2021).

[10] You, J. W., You, J., Weismann, M., and Panoiu, N. C., "Double-resonant enhancement of third-harmonic generation in graphene nanostructures," *Philos. Trans. R. Soc., A* **375**, 20160313 (2017).

[11] Ren, Q., You, J. W., and Panoiu, N. C., "Large enhancement of the effective second-order nonlinearity in graphene metasurfaces," *Phys. Rev. B* **99**, 205404 (2019).

[12] Koshelev, K., Kruk, S., Melik-Gaykazyan, E., Choi, J.-H., Bogdanov, A., Park, H.-G., and Kivshar, Y., "Subwavelength dielectric resonators for nonlinear nanophotonics," *Science* **367**, 288–292 (2020).

[13] Koskinen, K., Czaplicki, R., Slablab, A., Ning, T., Hermans, A., Kuyken, B., Mittal, V., Murugan, G. S., Niemi, T., Baets, R., and Kauranen, M., "Enhancement of bulk second-harmonic generation from silicon nitride films by material composition," *Opt. Lett.* **42**, 5030–5033 (2017).

[14] Synopsys® (available at: www.synopsys.com).